Construction and Building Materials 329 (2022) 127102

Contents lists available at ScienceDirect

Construction and Building Materials

journal homepage: www.elsevier.com/locate/conbuildmat

# Viscoelasticity modelling of asphalt mastics under permanent deformation through the use of fractional calculus

M. Lagos-Varas [a,b,*], D. Movilla-Quesada [b,c], A.C. Raposeiras [b,d], D. Castro-Fresno [a], O. Muñoz-Cáceres [a,b], V.C. Andrés-Valeri [b], M.A. Rodríguez-Esteban [c]

[a] GITECO Research Group, University of Cantabria, Av. Los Castros, 39005 Santander, Spain
[b] Gi2V Research Group, Institute of Civil Engineering, Faculty of Engineering Sciences, University Austral of Chile, Valdivia, Chile
[c] Departamento de Construcción y Agronomía, Escuela Politécnica Superior de Zamora, Universidad de Salamanca, 49029 Zamora, España
[d] Departamento de Ingeniería Mecánica, Escuela Politécnica Superior de Zamora, Universidad de Salamanca, 49029 Zamora, España.

ARTICLE INFO

*Keywords:*
Rheology
Permanent deformation
Asphalt mastic
Filler/bitumen
Creep-recovery
Hydrated lime
Fly ash

ABSTRACT

This study focuses on the mechanical behaviour of asphalt mastic composed of filler particles bonded with an asphalt bitumens. Asphalt mastics are viscoelastic composite materials widely used in the construction of pavement layers. The mechanical properties and the influence of the fillers on the filler/bitumen (f/b) matrix is one of the main areas of current research. In particular, the elastic determination of fillers for mechanical testing in asphalt mastic is relevant to understand permanent deformation caused by temperature variations caused by seasonal changes and vehicular traffic loads. In this sense, this research proposes a new methodology for rheological characterization of the elastic properties of the filler $\xi_2$ and elastic-viscous properties of the asphalt bitumen, $\xi_1$ and $\eta$, respectively, complementing the existing designs of asphalt mixture. The proposed methodology allows for identification of the influence of non-conventional fillers in the behavior of the asphalt mastic for the different recovery cycles of the Multiple Stress Creep Recovery (MSCR) and determination of new rheological parameters for the compression of the recovery phenomena and the elastic capacity of the type of filler and weight of the base bitumen. The results obtained show a greater adjustment to the experimental curves in determining the elastic modulus in each cycle for the hydrated lime and fly ash fillers with different filler/bitumen ratios. In particular, the proposed model for bituminous mastics achieves a strong fit with the experimental curves by empirically reducing the quadratic error ($R^2 = 0.99$) and managing to differentiate the elastic capacity $\xi_2$ of each filler and its effect with increasing concentration. For example, it establishes that the Hydrated lime filler (HL) acquires an average Young's modulus of 0.005 MPa, being 99.31% more elastic than Fly ash filler (FA) for a load of 3.2 kPa at a 1.25f/b ratio. In addition, the new model can be used to modify bitumen properties to design optimized and stronger asphalt mixtures.

## 1. Introduction

The asphalt mixture a composite of aggregates (coarse and fine aggregates), asphalt bitumen, air and possibly additive and modifying components [1,2]. These materials form a system in which the aggregate enveloped by a continuous film of asphalt bitumen [3]. The filler, whose particle size is less than 0.063 mm (according to EN 13043), is trapped by the asphalt bitumen, forming the asphalt mastic, which favours the agglomeration of the larger aggregates and influencing the properties of hot mix asphalt (HMA) [4].

In the last decades, the rheological study of the filler/bitumen (f/b) interaction has been relevant to know the properties that most influence the asphalt pavement, allowing the study of failures such as rutting and irregularities in the road surface, which cause premature deterioration of the pavement and a reduction in traffic comfort and safety [5,6]. The rheological analysis of the materials that compose the asphalt mixtures allows demonstrating, through the f/b interface, that the mastic has a high rutting resistance, even allowing improving the skid resistance, reducing the rolling noise and increasing the life cycle of the pavement.

The filler plays a fundamental role in this regard, since, due to its high specific surface area, it can withstand the stresses caused by internal friction or by contact between particles [7]. The characteristics of

* Corresponding Author.
*E-mail address:* manuel.lagos@uach.cl (M. Lagos-Varas).

https://doi.org/10.1016/j.conbuildmat.2022.127102
Received 1 November 2021; Received in revised form 25 February 2022; Accepted 8 March 2022
Available online 15 March 2022

**Table 1**
Characteristics of the asphalt bitumen B50/70.

| Properties | Standard | Results |
|---|---|---|
| Penetration at 25 °C (0,1 mm) | EN 1426 | 57.00 |
| Softening point (°C) | EN 1427 | 51.60 |
| Frass breaking point (°C) | EN 12,593 | −13.00 |
| Density (g/cm$^3$) | EN 15,326 | 1.035 |

the filler, such as morphology, composition, friction between particles, behaviour under humidity and temperature, generate physicochemical properties that develop a high degree of interaction with the bitumen, improving the mechanical behaviour of the mastic. The main fillers used as the mineral skeleton of the mastic are limes [8], fly ash [9], hydrated lime [10], slags [11], and others.

However, the most commonly used filler is limestone, due to the positive impact it has on the durability of asphalt mixtures, reducing the appearance of cracks caused by the effect of water and temperature variations.

The limestone filler (denoted as "L") increases the stiffness of the asphalt mixture and reactivates the asphalt bitumen, improving the adhesiveness between the aggregate-bitumen system [12]. Similarly, the use of hydrated lime (referred to as "HL") as a filler in asphalt mastics increases the mechanical strength of the asphalt mixture, minimizing the appearance of cracks [13], ageing and increasing the stiffness of the mastic [14]. In addition, when the HL has a degree of compatibility with the asphalt bitumen, a molecular layer is absorbed that positively affects the rheology of the mastic at high temperatures and to a greater degree if compared with inert fillers [15]. Likewise, HL filler improves the adhesiveness between the bitumen and the aggregate surface in an asphalt mixture, due to the water-insoluble salts generated by the precipitation of calcium ions, which prevents premature separation of the aggregate-bitumen interface [16].

On the other hand, results obtained in previous research have shown that the use of construction and demolition wastes (CDWs) and/or industrial and commercial by-products in asphalt mixtures is a good alternative from a sustainable (social, economic and environmental) point of view [17]. For example, fly ash (FA) is an industrial waste widely used as an environmentally friendly filler in asphalt mixtures. These fillers provide greater elasticity compared to limestone filler, improving the flexibility of the asphalt pavement. In addition, they have a significant impact on the viscosity and rheological properties of asphalt mastics, thus affecting the final strengths of asphalt mixtures [18].

According to the Marshall parameters for dense asphalt mixtures, the addition (up to 4%) of FA as a replacement for HL results in a 7.5% reduction in the optimum asphalt bitumen content, which minimizes the production cost of large-scale asphalt mixtures [19].

In 2017, researchers Li *et al.* [20] evaluated the thickness of the absorbing film between the filler and the asphalt bitumen, as it is an indicator of the physicochemical interaction and rheological properties of the asphalt mastic. The results showed that the FA filler has a thicker absorbed film compared to that of the HL filler, with those generated by L having a thinner film.

The asphalt bitumen has a rheology that determined by viscoelastic behaviour, to which elastic and viscous deformations are assigned [21,22]. Currently, the study of these deformations analyzes using its capacity to transform elastic-viscous states, under static and dynamic loads [23,24]. The mechanical characterization of the asphalt bitumen is achieved from classical methodologies of linear viscoelasticity, or techniques based on the damage resistance characterization. Classical methodologies allow the determination of softening, penetration points, brittleness, viscosity, among others, at a single temperature point [9]. However, current methods are based on the total deformation resistance and its relationship between the elastic and viscous parts of the asphalt bitumen [25].

The SUPERPAVE methodology allows the analysis of the rheological behaviour of asphalt bitumen and asphalt mixtures for a wide range of temperatures and loading frequencies [26]. In particular, this methodology establishes the parameter "$|G^*|/\sin(\delta)$" for the study of permanent deformations at elevated temperatures, determining a limit of the vulnerability of the asphalt bitumen to rutting failures [27]. However, several authors have stated that this parameter only considers linear viscoelastic (LVE) rheology [28], which does not effectively represent permanent deformation, since in asphalt mixtures this anomaly occurs in a nonlinear viscoelastic range. Thus, to identify a plasticity index that describes the rutting damage caused by the trajectory of the tire in the asphalt mixture, the Federal Highway Administration (FHWA) proposed to study the performance of asphalt bitumens for intermediate-high temperatures using the multiple stress creep recovery test (MSCR) [29].

The MSCR test generates stresses from multiple creep and recovery phenomena by evaluating the non-recoverable creep compliance ($J_{nr}$) [30] and the mean percentage recovery ($R$), which show the potential rutting rate and elasticity of the asphalt bitumen, respectively [31]. Creep and recovery phenomena generate in static cycles with controlled times [32]. Creep occurs in the process of specimen loading, which generate recoverable and non-recoverable strain states for non-linear viscoelastic deformations [1]. Subsequently, the recovery phenomenon details the capacity of the asphalt bitumen to redeem the deformations obtained in the creep process, determining the degree of plasticization in each cycle [33]. In addition, these parameters can reflect the rutting resistance of the asphalt mastic, where the load of 3.2 kPa is the one that generates a more accurate correlation to the permanent deformations in asphalt mixtures [34].

However, this methodology does not quantify the elastic capacity or Young's modulus of the type of filler used, nor does it allow evaluating a degree of softening of the f/b, as a measure of viscoelastic transition for a given temperature. Therefore, the application of a rheological model proposes, which establishes a set of springs and fractional dampers, representing a mineral aggregate particle (filler) with an agglomeration of the asphalt bitumen, to understand the rheology exhibited by the asphalt mastic, filler and bitumen jointly and/or independently. In this sense, the use of the mathematical equations of the proposed model allows detailing the viscoelastic transitions of the asphalt bitumen, quantifying the elastic capacity of the filler used and its relationship with the f/b dosage by means of the MSCR recovery phenomena [35].

The objective of this study is to establish the influence of fillers made up of HL, FA and L on the viscoelastic behaviour of asphalt mastic based on a rheological characterization of the filler/bitumen matrix by means of different loading rate, temperature, and dosage conditions. The study provides a new methodology to characterize the recovery phenomenon for each cycle of the MSCR test, knowing that the proposed model determines the degree of viscoelasticity and mechanical properties of the materials [1,35]. The application of the model establishes the Young's modulus of HL, FA and L for different dosage percentages (f/b 0.50, 0.75, 1.00 and 1.25) with respect to the weight of the base asphalt bitumen.

## 2. Materials and methods

### 2.1. Asphalt bitumen and mastic

In this study, the conventional asphalt bitumen B50/70 was used, whose classic mechanical properties summarized in Table 1 with the essential characteristics and specifications.

The fillers used for the manufacture of asphalt mastics are: HL, FA and L (Fig. 1). The aggregates use mostly used in wearing courses due to their mechanical properties, guaranteeing the necessary surface texture for some time. In addition, it is known that HL and L fillers possess a high content of calcium oxide (CaO) at 90.67% and 88.65%, respectively [36,37]. Leaving other main components such as silicon dioxide ($SiO_2$) and magnesium oxide (MgO) in second place [36]. FA have high $SiO_2$


**Fig. 1.** The fillers used sifted through an N°200 (0.08 mm) sieve. a) HL; b) FA; c) L.

**Table 2**
Physical and geometric properties of the fillers.

| Properties | Hydrated lime (HL) | Fly ash (FA) | Limestone (L) |
|---|---|---|---|
| Density (g/cm$^3$) | 1.959 | 2.450 | 2.725 |
| Rigden voids (%) | 76 | 73 | 74 |
| Granulometric analysis (%) | | | |
| Sieve (mm) | % Passed Through | | |
| 0.063 mm | 98.65 | 97.65 | 81.28 |
| 0.050 mm | 76.90 | 72.77 | 39.81 |
| 0.040 mm | 63.94 | 62.69 | 24.42 |
| 0.032 mm | 46.21 | 37.65 | 7.86 |
| 0.020 mm | 21.58 | 11.60 | 0.17 |

content between 43.53 and 60.31% depending on their nature [38], in addition to other compounds such as CaO and $Al_2O_3$ to a lesser extent [39].

The characterization of the basic properties (see Table 2) of the fillers used based on the determination of particle density by the pycnometer method according to EN 1097–7. In addition, the content of Rigden voids (RV) was calculated based on the EN 1097–4 procedure from the density obtained.

The manufacturing process of the asphalt mastics is carried out by mixing the base bitumen type B50/70 with the fillers of HL, FA and L, independently. Several samples are generated based on the filler/bitumen (f/b) dosage for each of the fillers mentioned. The f/b ratios in a mass of base bitumen are 0.50, 0.75, 1.00 and 1.25. Additionally, B50/70 base bitumen samples prepared for the analysis of reference samples.

As for the fabrication of the samples, the B50/70 base bitumen was heated in an oven at 153 °C for 2 h until medium aging was achieved in an asphalt mix (Fig. 2). In addition, the fillers used were heated at a temperature of 170 °C for four hours to create mastic samples under the same conditions as those obtained in an asphalt mix. The mastic samples were not aged using the Rolling Thin Film Oven Test (RTFOT) as it is indicated in the AASHTO M 332 since the objective is to simulate the recovery curves of asphalt mastics for the classification of filler elasticity and bitumen viscoelasticity, and that these mastics are equivalent to those of asphalt mixtures manufactured in the laboratory.

Subsequently, a portion of the dosed mass of the asphalt bitumen was deposited in a mixer homogenizer at 153–154 °C. The previously prepared fillers of HL, FA and L are added individually to the base bitumen for each dosage slowly for better homogenization. The speed and time of manufacture vary in prior art studies depending on digestion and/or air removal in homogenization (5–30 min and 500–4500 rpm). The HL charge with the highest dosage (f/b = 1.25) was used as a reference in digestion time and speed because it has the highest mass concentration. Therefore, a manufacturing process at 1500 rpm in about 10–15 min was defined, which is within the actual process. Finally, the homogeneous mixture is deposited in the 8 and 25 mm molds standardized for testing in the dynamic shear rheometer (DSR), obtaining 13 different types of asphalt mastic samples.

### 2.2. Mechanical properties of linear viscoelasticity

The linear viscoelastic properties of asphalt bitumen and mastics are determined by the DSR-test methodology, applying the master curve fitting for the complex modulus $|G^*|$ and angle of phase $\delta$ [40,41].

The values of the $|G^*|$ vector and angle $\delta$ are obtained using two parallel plates of known geometry. El The temperature sweep of the test extends from 10 °C to 70 °C. A 25 mm parallel plate is used for the 30 to 70 °C temperature range, and an 8 mm parallel plate used for the 10 to

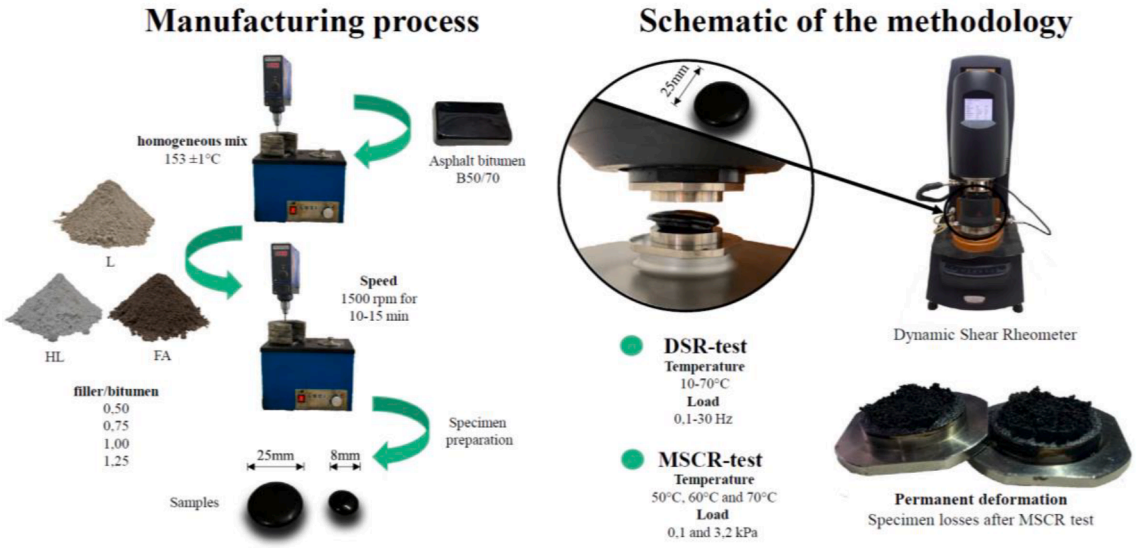


**Fig. 2.** Schematic of the manufacture and methodology for determining the rheological properties of asphalt mastics.

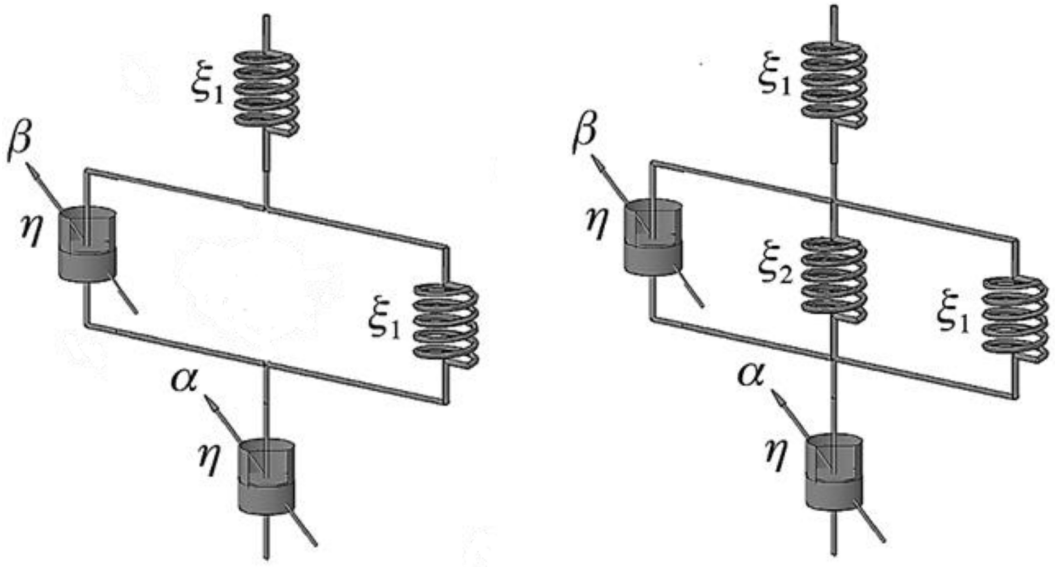


**Fig. 3.** Schematic diagram of the rheological models. a) Asphalt bitumen; b) Asphalt mastic.

30 °C range. The 30 °C temperature averaged for the two ranges with a difference of less than 5%. The oscillating model of the test is performed for 10 frequencies in a range from 0.1 to 30 Hz, with a sinusoidal displacement of 0.1% strain.

The master curves used to understand the susceptibility between temperature and load frequency variables in two dimensions. In the present study, a master curve fit by time–temperature superposition [42] is used for the values of $|G^*|$ and $\delta$, from the test frequencies and temperatures (10 to 70 °C), converging to a single curve approximated by the sigmoidal function (see Eq. (1)).

$$\log(G^*) = \alpha + \frac{\lambda}{1 + e^{\varphi - \gamma \cdot \log(\omega_r)}} \tag{1}$$

Where, $\alpha$ is the lower asymptote, $\lambda$ is the difference between the upper and lower asymptote values, $\varphi$ is the inflexion point, $\gamma$ is the slope, and $\omega_r$ is the reduced frequency.

An index ($I_{mastic}$) has been defined to provide an interpretation of the results and quantify the variation of the mass increase on the fillers. The variable $I_{mastic}$ (see Eq. (2)) is only a proposed indicator to obtain the ranges of possible values of $G^*$ caused by the type of filler for $\omega_r$. The objective is only to calculate the maximum and minimum value of $G^*$ when varying the concentration, with respect to its lower dosage. The theoretical foundation is based solely on the time–temperature superposition principle, defined by Eq. (1) for the extreme concentrations (f/b 0.50 and 1.25). The difference of the area under the curve is calculated by means of an integral defined and calculated with MATLAB© for each curve, obtaining a stiffness domain by type of filler used.

$$I_{Mastic} = \int_{\alpha}^{\alpha+\lambda} \left[ \log \frac{G^*\left(\omega_{r,f/b=1.25}\right)}{G^*\left(\omega_{r,f/b=0.50}\right)} - \log G^*\left(\omega_{r,f/b=0.50}\right) \right] d\omega_r \tag{2}$$

Where $G^*$ is the complex modulus, $\omega_r$ is the reduced frequency for each dosage f/b between the integral limits of the sigmoidal curve.

### 2.3. Damage resistance characterization mechanical properties

#### 2.3.1. MSCR test

In this study, the MSCR test performed for the base bitumen and asphalt mastics at a test temperature of 50 °C, 60 °C and 70 °C by performing 20 continuous loading and unloading cycles with 25 mm diameter plate on the DSR (AASHTO T 350). The load is set for a torque of 0.1 kPa to condition the specimens and then at 3.2 kPa to cause damage to the specimen.

The creep phenomenon set with a time of 1 s and the recovery extended 9 s. The two parameters of the MSCR test are non-recoverable compliance ($J_{nr}$) and percentage recovery (R) (AASHTO M 332). The above parameters establish criteria for evaluating yield strain and recovery capability of samples using Eqs. (3) and (4), respectively:.

$$J_{nr\sigma}(1/kPa) = \frac{1}{10} \sum_{i=1}^{10} \frac{\gamma_{n_i} - \gamma_{0_i}}{\sigma} \tag{3}$$

$$R_{\sigma}(\%) = \frac{1}{10} \sum_{n=1}^{10} \frac{\gamma_{p_i} - \gamma_{n_i}}{\gamma_{p_i} - \gamma_{0_i}} \tag{4}$$

where $\gamma_0$ represents the shear stress at the beginning of the cycle, $\gamma_p$ is the point of most significant deformation after 1 s of load, $\gamma_n$ represents the non-recoverable stress at the end of the first cycle, and $\tau$ represents the yield stress in each period. Thus, four parameters are obtained ($R_{0.1}$, $J_{nr0.1}$, $R_{3.2}$, and $J_{nr3.2}$) which indicate the standard mean of each phenomenon for the two load quantities.

### 2.4. Rheological models for bitumen and asphalt mastic

The rheological simulation of the MSCR based on a mechanical representation of the bitumen and mastic asphalt (Fig. 3), demonstrated for the viscoelastic deformations of the filler/bitumen system. The model defines the elastic property of the filler utilizing the variable $\xi_2$ (kPa), representing Young's modulus for each type of filler and its relationship with the dosage f/b. In the case of the asphalt bitumen, the variables $\xi_1$ (kPa) and $\eta$ (kPa·s) established for the elastic and viscous representation of the B50/70 base bitumen defined for each temperature and test load.

The Riemann-Liouville integral and fractional derivative of a function are defined as follows $f(t)$, in the Eqs. (5) and (6) respectively, to obtain the differential equation of the model [43]:.

$$D_t^{-\alpha} f(t) = \frac{1}{\Gamma(\alpha)} \int_0^t (t-u)^{\alpha-1} f(u) du, \alpha > 0, \tag{5}$$

$$D_t^{\alpha} f(t) = D^n D^{\alpha-n} f(t) = \frac{1}{\Gamma(n-\alpha)} \frac{d^n}{dt^n} \int_0^t \frac{f(u)}{(t-u)^{\alpha-n+1}} du, \alpha > 0, \tag{6}$$

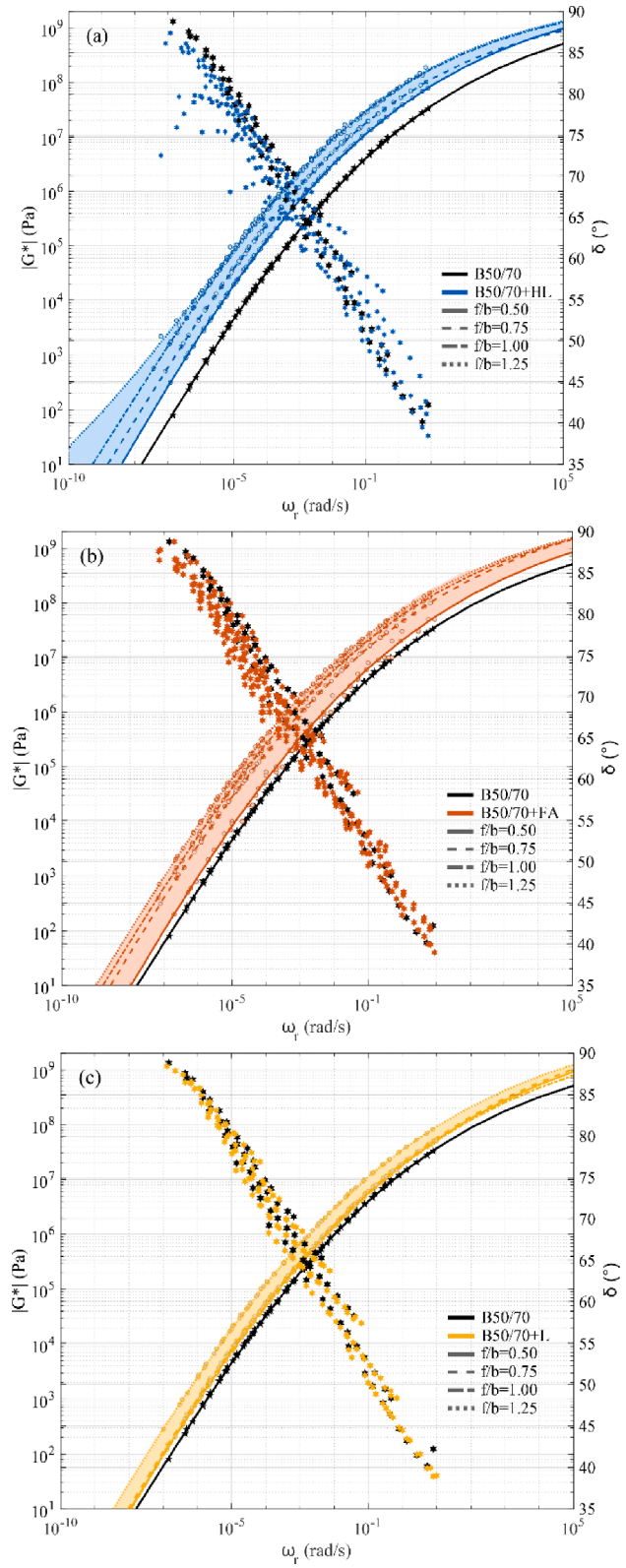


**Fig. 4.** Master curve of the $|G^*|$ and $\delta$ for asphalt mastics. a) HL; b) FA; c) L.

Where $n$ is a positive number, $n$-1 $\leq \alpha < n$, $t$ is time and $\Gamma(.)$ is the Gamma function. Particularly, when $\alpha = n$, then $D_t{}^{\alpha}f(t) = d^n/Dt^n f(t)$.

The differential equation governing the model for asphalt mastics is obtained after applying the above definition, based on the use of fractional calculus as it is shown in Eq. (7),. The mathematical development achieved by adding the unit deformations of the mechanical elements.

With this, the fractional derivatives α, β,y,γ are established, which have a range of possible values between 0 and 1, to satisfy the classical equations of the Maxwell and Kelvin-Voigt models [44]. By substituting and transforming the derivatives algebraically [1].

$$D_t^{\alpha+\beta}\epsilon(t)+\frac{M}{\eta}D_t^{\alpha}\epsilon(t)=\frac{1}{\xi_1}D_t^{\beta+\gamma}\sigma(t)+\frac{1}{\eta}D_t^{\beta}\sigma(t)+\frac{1}{\eta}D_t^{\alpha}\sigma(t)+\frac{M}{\xi_1\eta}D_t^{\gamma}\sigma(t)+\frac{M}{\eta^2}\sigma(t) \tag{7}$$

Where $\varepsilon(t)$ is the strain, $\sigma(t)$ is the stress, $M = \xi_1 + \xi_2$ y $D_t{}^{\alpha}$, $D_t{}^{\beta}$ and $D_t{}^{\gamma}$ are the fractional derivatives with respect to time $t$.

The recovery phenomenon begins when the initial 1 s MSCR-test stress is released, giving rise to a function that depends on time and material type. To describe this process, it is necessary to consider Eq. (7) by eliminating the concept of initial stress $\sigma_0 = 0$ resulting in the following definition [1]:.

$$\widehat{\epsilon}\left[s^{\alpha+\beta}-\sum_{k=0}^{m-1}s^{\beta+\alpha-k-1}\epsilon^k(0)+\frac{M}{\eta}s^{\alpha}-\sum_{k=0}^{m-1}s^{\beta-k-1}\epsilon^k(0)\right]=0 \tag{8}$$

Where α and β values between $m$-1 and $m$, $m$ is the positive number closest to the value of α and β. Having said this, and by means of the Mittag-Leffler ($E_q$) [45] with the argument -$at\alpha$, the following Laplace transform is defined:.

$$L\{E_{\alpha}[-at^{\alpha}]\}=L\left\{\sum_{K=0}^{\infty}\frac{(-at^{\alpha})^k}{\Gamma(k\alpha+1)}\right\}=L\left\{\sum_{k=0}^{\infty}\frac{(-a)^k t^{k\alpha}}{\Gamma(k\alpha+1)}\right\}=\frac{s^{\alpha}}{s(s^{\alpha}-a)}\alpha > 0 \tag{9}$$

After applying the above definition, the recovery function of the bitumen and asphalt mastic for the MSCR test is obtained in fractional form in Eqs. (10) and (11), respectively:.

$$R_{Bitumen}(t)=\epsilon_M^0(0)\sum_{k=0}^{\infty}\frac{\left(-\frac{\xi_1}{\eta}t^{\beta}\right)^k}{\Gamma(1+\beta k)}+\epsilon_{\infty}^0(0), \tag{10}$$

$$R_{Mastic}(t)=\epsilon_M^0(0)\sum_{k=0}^{\infty}\frac{\left(-\frac{M}{\eta}t^{\beta}\right)^k}{\Gamma(1+\beta k)}+\epsilon_{\infty}^0(0), \tag{11}$$

where $R_{Mastic}$ $(t)$ is the recovery strain for asphalt mastic, $R_{Bitumen}$ $(t)$ is the recovery strain for asphalt bitumen, $\Gamma(.)$ is the Gamma function, $\varepsilon_{\infty}{}^0(0)$ is the adjustment factor of the Maxwell's model [46], and $\varepsilon_M{}^0(0)$ is the adjustment factor of the parallel system and Mittag-Leffler infinite series, which depends on the parameter and which describes the visco-elastic transformation process $M = \xi_1 + \xi_2$, which is the elastic capacity of the bituminous mastic.

## 3. Results and discussion

### 3.1. Analysis of the dynamic modulus $|G^*|$ and phase angle $\delta$

Fig. 4 shows the master curves $|G^*|$ and the variation of the offset angle of the base bitumen and the asphalt mastics.

The results show that the mastics in their different f/b ratios generate a band of use characteristic of the stiffness capacity of the filler type. In particular, an increase in stiffness obtained for the three types of mastics (HL, FA and L) with increasing f/b concentration. For low temperatures or high reduced frequencies $\omega_r$, no major differences between the filler types observed, reaching an average stiffness of 109 Pa. On the contrary, for high temperatures or low reduced frequencies $\omega_r$, differences are observed in the samples due to the thermal susceptibility and the amount of mass per unit volume of the asphalt bitumen.

Samples with HL filler (Fig. 4a) have the highest stiffness compared to FA and L mastics in all $\omega_r$ and f/b ratio domains. At 10 °C the HL filler

**Table 3**
Parameters of a master curve for asphalt bitumen and mastics.

| Type | $I_{mastic}$ | $f/b$ | $\alpha$ | $\lambda$ | $\varphi$ | $\gamma$ | $a_1 \cdot 10^{-4}$ | $a_2$ | $a_3$ | $R^2$ |
|---|---|---|---|---|---|---|---|---|---|---|
| B50/70 | – | – | −7.32 | 16.86 | −1.79 | 0.23 | 7.18 | −0.15 | 0.0076 | 0.99 |
| B50/70 + HL | 40.59% | 0.50 | −8.89 | 18.70 | −1.97 | 0.22 | 7.04 | −0.15 | 0.0075 | 0.99 |
| | | 0.75 | −6.02 | 15.54 | −2.01 | 0.25 | 7.52 | −0.15 | 0.0075 | 0.99 |
| | | 1.00 | −5.80 | 15.47 | −2.04 | 0.25 | 8.64 | −0.16 | 0.0075 | 0.99 |
| | | 1.25 | −1.49 | 11.07 | −1.72 | 0.28 | 7.54 | −0.15 | 0.0076 | 0.99 |
| B50/70 + FA | 91.52% | 0.50 | −10.57 | 20.50 | −1.92 | 0.21 | 6.70 | −2.14 | 0.0075 | 0.99 |
| | | 0.75 | −10.40 | 20.50 | −2.00 | 0.21 | 7.73 | −0.15 | 0.0076 | 0.99 |
| | | 1.00 | −7.68 | 17.58 | −1.99 | 0.23 | 7.92 | −0.15 | 0.0075 | 0.99 |
| | | 1.25 | −7.69 | 17.58 | −2.04 | 0.23 | 7.78 | −0.15 | 0.0075 | 0.99 |
| B50/70 + L | 36.92% | 0.50 | −11.72 | 21.85 | −1.89 | 0.19 | 7.08 | −0.14 | 0.0076 | 0.99 |
| | | 0.75 | −11.70 | 21.91 | −1.87 | 0.19 | 6.89 | −0.14 | 0.0076 | 0.99 |
| | | 1.00 | −10.41 | 20.32 | −1.90 | 0.21 | 6.06 | −0.13 | 0.0076 | 0.99 |
| | | 1.25 | −9.54 | 19.60 | −1.91 | 0.21 | 7.13 | −0.14 | 0.0076 | 0.99 |

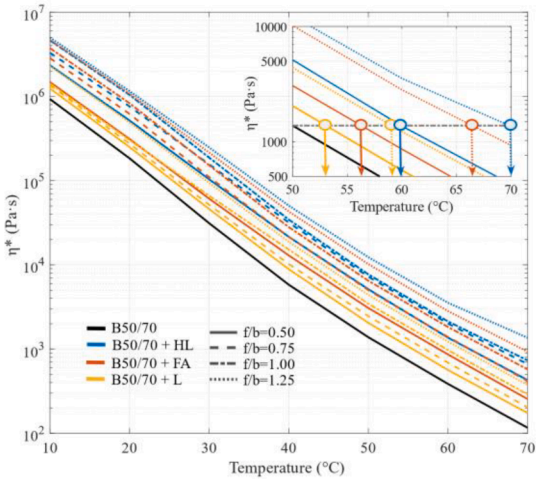


**Fig. 5.** Results of the complex viscosity of the bitumen and asphalt mastics.

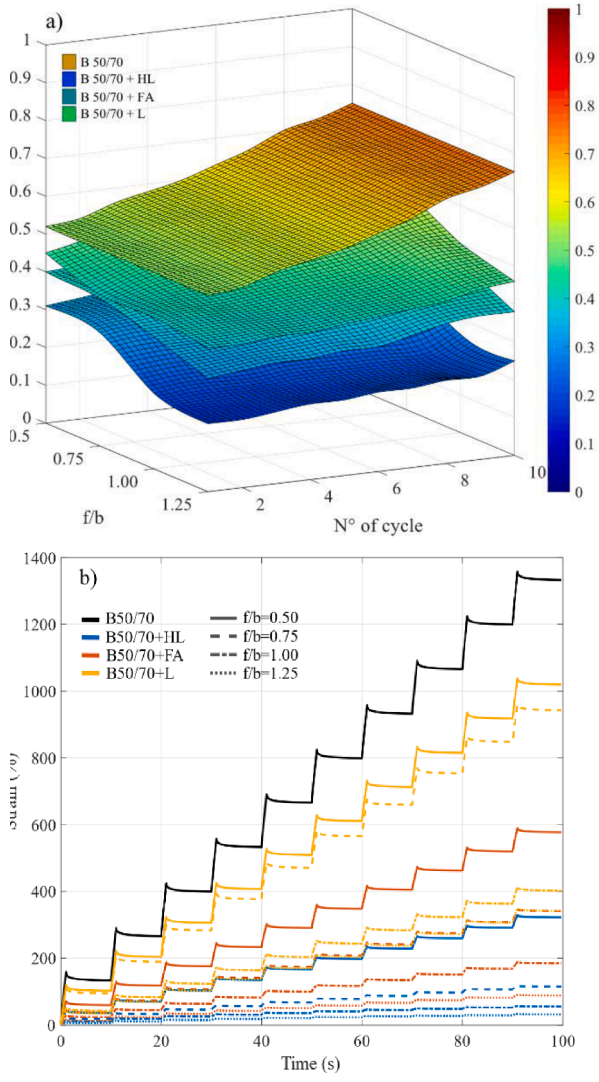


**Fig. 6.** MSCR-test at 50 °C. a) fractional exponent $\beta$; b) experimental strain for 3.2 kPa.

generates a stiffness of 49 MPa for the 1.25f/b ratio, which subsequently drops to 21.41–10-6 MPa, for the f/b ratio equal to 0.50 at a frequency of 1.59 Hz.

On the contrary, the samples with FA generate a maximum of 46 MPa for f/b equal to1.25, and consecutively decreases by 31 MPa, for the lowest dosage (f/b equal to0.50), generating a greater variation in the values of $|G^*|$, and causing a 16.54% difference compared to the HL filler.

This variation of the complex modulus $|G^*|$ product of the increase of the f/b ratio is produced due to the great stiffness capacity obtained by the HL filler, generating an inflexion point for lower $\omega_r$, due to the greater amount of fine particles that this filler has, compared to the FA filler (Table 2).

However, when comparing the rheological behaviour of FA with L filler, an increase in the difference in the values of the full modulus ($|G^*|$) at a temperature of 10 °C is obtained. The fly ash mastics generate 66.69% higher stiffness compared to the L mastic. As the temperature increases (70 °C), the values of $|G^*|$ increase without a large variation between the fillers, generating a parallel growth to that produced by the B50/70 type bitumen (Fig. 4b and 4c).

On the other hand, when fitting the curves by means of the sigmoidal function and determining the $I_{mastic}$ index (see Table 3), it is obtained that mastics with HL have a higher stiffness |G*| per mass-volume amount of the samples. The mastics with FA define a band of use with a larger area than the other fillers with a growth of 91.52%, being more susceptible to variations in temperature and loading frequencies. The mastics with filler L generate a difference in the values of the complex modulus |G*| of 36.92%, on the variation of the dosage f/b. Finally, the mastics with filler HL generate a band of use with a growth of 40.59% over the dosage of F/B 0.50. This slight difference of HL is due only to the rheological capacity it acquires at elevated temperatures, being the only type of filler that reaches a stiffness of 108 Pa for r of the order of 10–10 rad/s.

Referring to the output data of Eq (1), a growth of 10 Pa is obtained

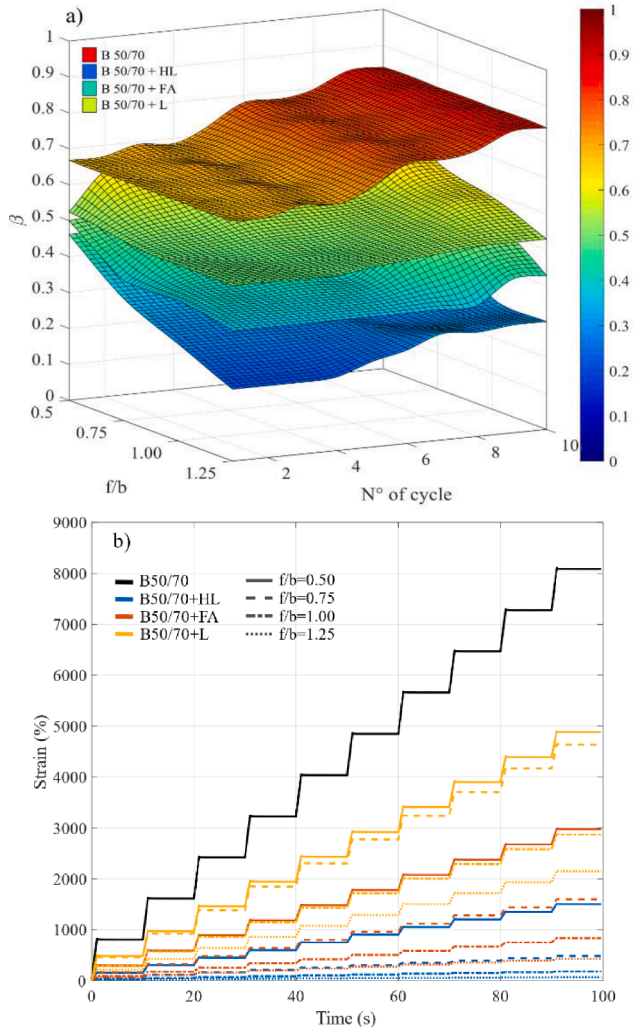


**Fig. 7.** MSCR-test at 60 °C. a) fractional exponent $\beta$; b) experimental strain for 3.2 kPa.

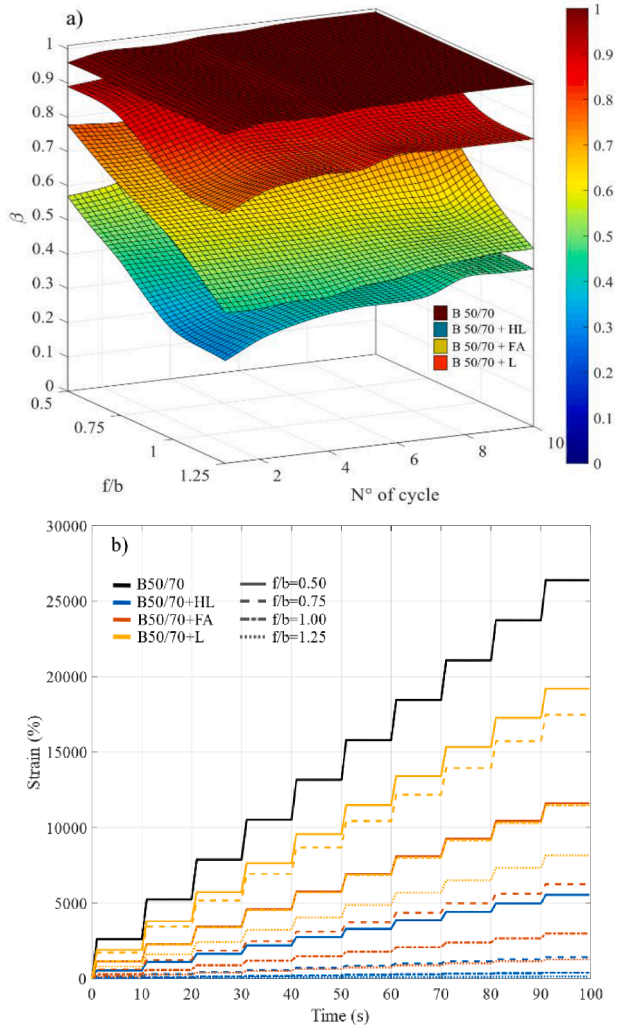


**Fig. 8.** MSCR-test at 70 °C. a) fractional exponent $\beta$; b) experimental strain for 3.2 kPa.

as the arithmetic mean between the upper and lower asymptotes of all samples. The inflexion point is shifted to the right for the r values by adding FA filler, HL and L. The slope of the sigmoidal curve is directly proportional to the amount of filler placed in the mixture, generating higher values of $|G^*|$ at lower $\omega_r$.

Fig. 5 shows the complex viscosity $\eta^*$ of bitumen type B50/70 and asphalt mastics. The results show that the complex parameter decreases as the experimental temperature decreases, which is caused by the softening of the material and the reduction of its stiffness.

The addition of the different types of fillers shifts the bitumen standard curve to the right, allowing higher values $\eta^*$ for any reference temperature. In particular, mastics with Lfiller have the lowest changes compared to HL filler and FA. The data show that for a reference viscosity of the bitumen at a temperature of 50 °C, the same value is obtained at 53.0 °C, 54.5 °C, 57.2 °C and 59.2 °C for f/b dosages equal to 0.50, 0.75, 1.00 and 1.25, respectively for the L filler.

The mastics with FA present (for the same reference) a shift to the right up to temperatures of 56.3 °C, 60.0 °C, 62.4 °C and 66.9 °C for the proposed f/b increment, generating growth of 62.90% for the possible values of $\eta^*$ about the L filler.

Finally, the mastics with HL filler are the ones that present the greatest differences about the standard curve of the B50/70 type bitumen. The results determined that for the f/b concentration equal to 0.5, a temperature of 59.9 °C is obtained about the $\eta^*$ value at 50 °C of the B50/70 type bitumen. The f/b concentrations equal to 0.75, 1.00 and 1.25 of HL filler reach temperatures of 60.0 °C, 62.40 °C and 70.0 °C, respectively. This increase in temperature determines an increase of 70.97% compared to the values obtained with L filler for f/b ratios 0.5–1.25.

**Table 4**
Elasticity parameter $\xi_2$ (kPa) for asphalt mastics.

| Type | f/b | Temperature | | |
|---|---|---|---|---|
| | | 50 °C | 60 °C | 70 °C |
| B50/70 + HL | 1.25 | $4.70{\cdot}10^{-3}$ | $4.65{\cdot}10^{-3}$ | $4.70{\cdot}10^{-3}$ |
| | 1.00 | $6.00{\cdot}10^{-4}$ | $5.80{\cdot}10^{-4}$ | $6.00{\cdot}10^{-4}$ |
| | 0.75 | $1.00{\cdot}10^{-5}$ | $1.00{\cdot}10^{-5}$ | $1.00{\cdot}10^{-5}$ |
| | 0.50 | $2.00{\cdot}10^{-14}$ | $2.25{\cdot}10^{-14}$ | $2.00{\cdot}10^{-14}$ |
| B50/70 + FA | 1.25 | $3.00{\cdot}10^{-5}$ | $3.19{\cdot}10^{-5}$ | $3.00{\cdot}10^{-5}$ |
| | 1.00 | $1.00{\cdot}10^{-5}$ | $1.08{\cdot}10^{-5}$ | $1.00{\cdot}10^{-5}$ |
| | 0.75 | $1.01{\cdot}10^{-6}$ | $1.10{\cdot}10^{-6}$ | $1.00{\cdot}10^{-6}$ |
| | 0.50 | $2.00{\cdot}10^{-14}$ | $3.16{\cdot}10^{-14}$ | $2.00{\cdot}10^{-14}$ |
| B50/70 + L | 1.25 | $2.16{\cdot}10^{-7}$ | $2.15{\cdot}10^{-7}$ | $2.16{\cdot}10^{-7}$ |
| | 1.00 | $5.00{\cdot}10^{-12}$ | $1.46{\cdot}10^{-12}$ | $1.40{\cdot}10^{-12}$ |
| | 0.75 | $2.17{\cdot}10^{-12}$ | $2.16{\cdot}10^{-12}$ | $2.17{\cdot}10^{-12}$ |
| | 0.50 | $4.42{\cdot}10^{-14}$ | $4.42{\cdot}10^{-14}$ | $4.40{\cdot}10^{-14}$ |

**Table 5**
Anova for $\xi_2$.

| Source of variability | Sum of squares | Degrees of freedom | Mean squares | F-statistic | P-value |
|---|---|---|---|---|---|
| B50/70 + HL | 0 | 2 | $3.66307 \cdot 10^{-9}$ | 0 | 0.9993 |
| Error | 0.00059 | 117 | $5.08114 \cdot 10^{-6}$ | – | – |
| Total | 0.00059 | 119 | – | – | – |
| B50/70 + FA | $1.39096 \cdot 10^{-11}$ | 2 | $6.95479 \cdot 10^{-12}$ | 0.04 | 0.9564 |
| Error | $1.82610 \cdot 10^{-8}$ | 117 | $1.56077 \cdot 10^{-10}$ | – | – |
| Total | $1.82749 \cdot 10^{-8}$ | 119 | – | – | – |
| B50/70 + L | $3.9103 \cdot 10^{-9}$ | 2 | $1.95515 \cdot 10^{-19}$ | $8.81016 \cdot 10^{-6}$ | 0.9999 |
| Error | $2.59646 \cdot 10^{-12}$ | 117 | $1.95551 \cdot 10^{-14}$ | – | – |
| Total | $2.59646 \cdot 10^{-12}$ | 119 | – | – | – |

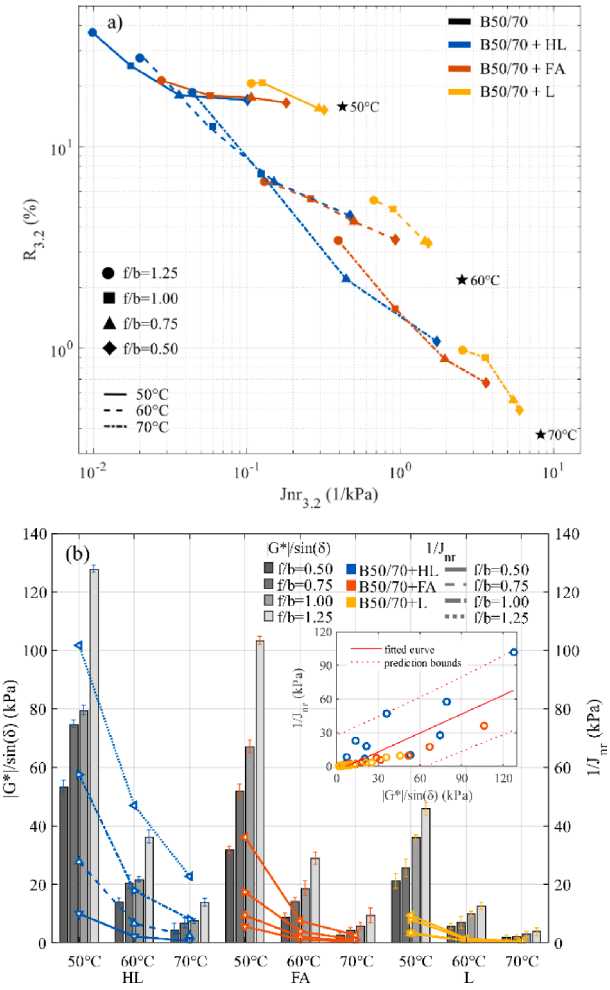


**Fig. 9.** MSCR values of asphalt mastics with different f/b ratio. a) $J_{nr3.2}$ v/s R values; b) $|G^*|/\sin(\delta)$ and $J_{nr3.2}$ values.

### 3.2. Experimental analysis of the MSCR test

The deformations that appear when asphalt bitumen and mastic specimens subjected to creep and multiple recovery phenomena allow quantifying the contribution of the type of filler used and its relation with the bitumen mass. Therefore, it is possible to detail the rheological properties of the asphalt mastic by applying the model proposed, including the viscoelastic transition during the MSCR-test, which could cause permanent deformations in asphalt mixtures (see Appendix A).

Fig. 6 shows the non-linear viscoelastic behaviour of the samples for a temperature of 50 °C. The experimental data obtained show that bitumen type B50/70 presents an accumulated deformation of 1333.1%. However, when adding filler to this sample, it is determined that the L filler presents the highest deformations reaching a range of 341.34–1019.90% of accumulated deformation for the variation of f/b 0.50–1.25. Regarding the samples with FA filler a domain of 88.58–577.73% is reached presenting a percentage difference of 43–74% of better mechanical performance, compared to the L filler for the same variation. Finally, mastics with HL present the best performance recovering a large part of the deformation. The values oscillate between 31.45 and 322.63% of accumulated deformation defining an improvement of 68–91% in reference to the L filler for the limits f/b 1.25–0.50, respectively.

To perform the mathematical adjustment of Eqs. (10) and (11) a computer code is developed. The results (see Fig. 6a) demonstrate the elastic influence of the type of filler used and its relation to the f/b dosage. First, the fit is established by Eq. (10) which indicates the characterization of the viscoelastic deformations of the bitumen type B50/70. The fractional exponent $\beta$ demonstrates the viscoelastic transition of bitumen type B50/70 since when this value is 0, the material under study is considered a completely elastic solid, while if it reaches the maximum value ($\beta$ equal to1), the material is considered a Newtonian fluid.

In Fig. 6a, it is observed that the bitumen type B50/70 at a temperature of 50 °C reaches $\beta$ 0.52 for the first cycle of the MSCR at 3.2 kPa. Subsequently, for the last test cycle, this value increases to a maximum $\beta_{máx}$ of 0.75, demonstrating the multiple stress softening capacity of bitumen type B50/70.

Subsequently, when adjusting the rheological model Eq. (11) for asphalt mastics, lower values $\beta$ are reached due to the elastic capacity of the filler, which delays the state of deformation mentioned. The samples with the lowest values $\beta$ are those with HL filler, reaching a maximum value of 0.38, which drops sharply as the filler concentration increases above the f/b dosage equal to 1.00 (see Fig. 6a). L and FA mastics have higher $\beta$ values than those of HL, with a linear decrease of the parameter as the f/b ratio increases. The maximum values $\beta$ obtained for the filler surfaces with FA and L are 0.53 and 0.65 for the maximum dosage, respectively.

Increasing the temperature up to a temperature of 60 °C generates a greater difference in the results between the bitumen and mastics compared to those obtained at 50 °C. Fig. 7b shows that bitumen type B50/70 reaches 8084.6% deformation, generating a considerable increase in the viscoelastic transition with respect to the 50 °C temperature. For the viscoelastic simulation criteria, bitumen type B50/70 at 60 °C (see Fig. 7a), reaches a maximum value of $\beta = 0.84$ for the tenth cycle of the test, reaching a growth of 12% compared to the previous temperature.

Mastics with L filler show the highest deformations among the types of filler studied. The range of deformations is 2149–4882%, generating a softening product of multiple stress with value $\beta$ of 0.48–0.76, increasing by 16% the values for the variation of f/b equal to 0.5–1.25. In addition, mastics with FA fillers present a range of 429–2974%, improving the behaviour compared to samples with L by 43–80% for f/b dosages equal to 1.25 to 0.50. The above shows that there are no differences in the behaviour shown by the mastics at a temperature of 50 °C between FA and L. Likewise, the mastics with FA increase the viscoelastic transition $\beta$ by 11% in reference to the 50 °C temperature, demonstrating greater elasticity than those made with L.

Finally, the samples with HL show the best behaviour under creep-recovery phenomena with a domain of 68–1503% of accumulated deformation. Similarly to the samples with FA, the mastics with HL

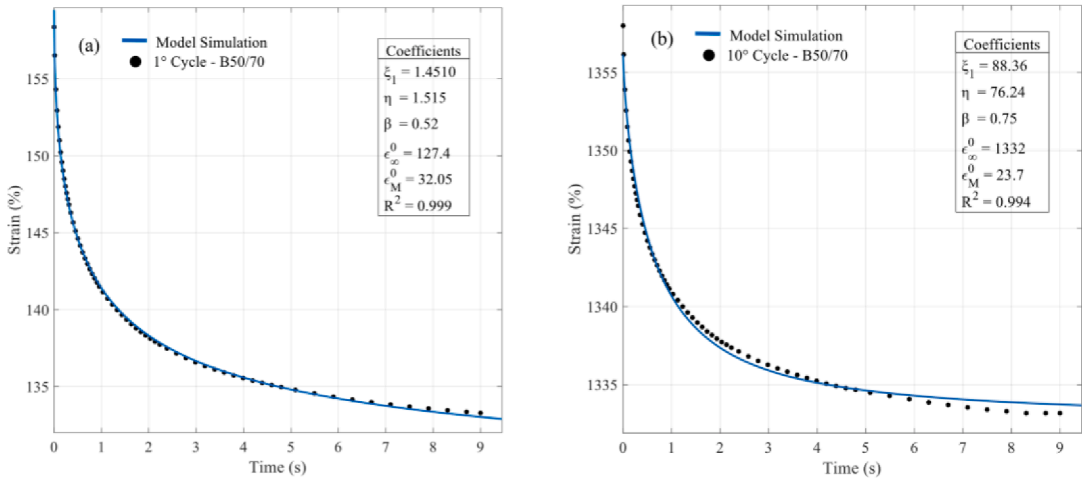


**Fig. 10.** Rheological simulation of bitumen B50/70 for 3.2 kPa and 50 °C. a) 1°cycle; b)10°cycle.

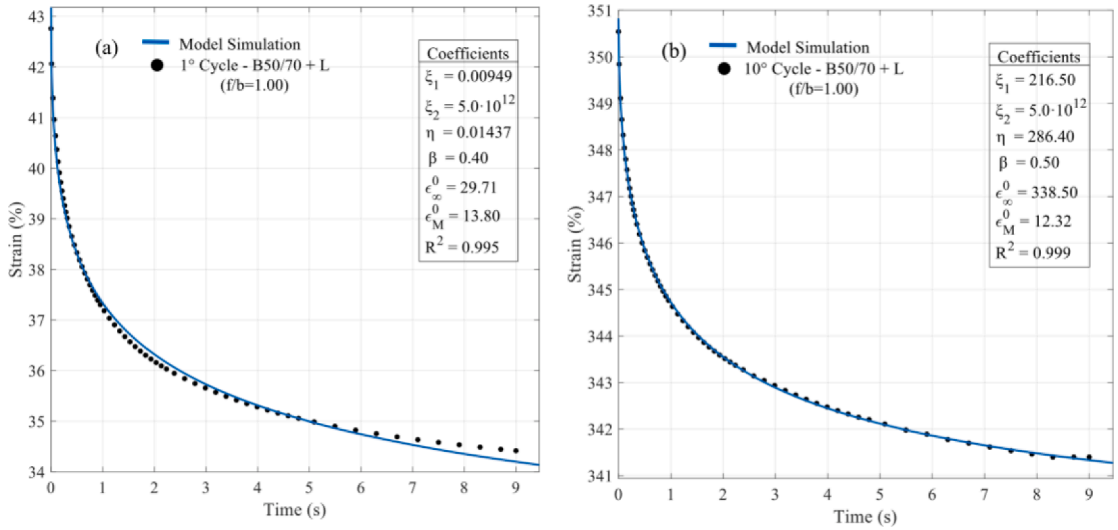


**Fig. 11.** Rheological simulation of limestone asphalt mastic for 3.2 kPa and 50 °C. a) 1°cycle; b)10°cycle.

maintain the percentage difference obtained at 50 °C, defining an improvement of 69–91% in relation to the behaviour of the samples with L.

The domain $\beta$ for the samples with HL extends from 0.20 to 0.50, generating a behaviour with a higher tendency to elasticity ($\beta = 0$) compared to FA and L. In contrast to the rheological simulation at 50 °C, the samples with HL generated the greatest changes with 28% of the increase $\beta$.

Fig. 8 shows the rheological behaviour of the bitumen and asphalt mastics for a temperature of 70 °C in the MSCR test. Bitumen type B50/70 is the sample with the highest deformation (26389% accumulated; the rheological simulation (see Fig. 8a) shows that the rheological values $\beta$ reach a minimum value of 0.96 for the first cycle, reaching the maximum value of $\beta = 1$, demonstrating a Newtonian fluid behaviour.

The samples with L filler acquire a deformation range from 8164% to 19205%, with an increase $\beta$ of varying between 0.72 and 0.96 for the variation of f/b equal to 0.5–1.25. The mastics with FA present a deformable range of 1261–6255%, which increases the range obtained at a temperature of 60 °C, obtaining an improvement in the performance of 40–84%, compared to the samples with L, for the range of f/b equal to 1.25 to 0.50. The transition of the parameter $\beta$ for the samples with FA ends in an interval 0.44–0.95, which shows a maximum growth of 36% for the f/b ratio equal to 0.50.

The HL filler generates the best performance when mixed with bitumen type B50/70 compared to the rest of the fillers. The results indicate a domain of 140–5539% of accumulated deformation, being 71% more efficient than the L samples for f/b equal to 0.50, and reaching 98% for the dosage of f/b equal to 1.25. With respect to the normalization of the vector $\beta$, a final domain is obtained for HL mastics at 70 °C from 0.30 to 0.78, being the filler that generates the highest elasticity.

In addition to the degree of viscoelasticity obtained with the fractional derivative $\beta$, the proposed model for mastic asphalt (Fig. 3b) allows detailing the elastic capacity $\xi_2$ of the different fillers, due to the infinitesimal representation of the mineral aggregate enveloped by the asphalt bitumen. The results (Table 4) determine that for the 10 cycles of the MSCR at 3.2 kPa, the elastic property $\xi_2$ increases as a higher concentration of filler is added to the sample.

In particular, when comparing the types of fillers, it is observed that a higher Young's modulus is quantified for the samples with HL in the four dosages analyzed. This elastic difference is greater for the filler/bitumen ratios with higher filler content, demonstrating that the mathematical adjustment allows detailing the elasticity as a function of the nature of the filler and its relation to the mass of the asphalt bitumen.

In this sense, the samples with HL filler present a greater elastic difference of 4.67–10-3 kPa for the highest f/b concentration at 50 °C.

Subsequently, this difference decreases with decreasing filler content, reaching 5.9–10-4 kPa for f/b ratio equal to 1.00 and 9.00–10-6 kPa for f/b ratio equal to 0.75. Otherwise, the model is not able to predict a difference for the f/b concentration equal to 0.50 between the HL and FA fillers, characterizing the same Young's modulus for 50 °C, which is due to the similarity of the mechanical behaviour for low concentrations.

When analyzing the L filler, it is observed that the model shows even lower values than those obtained with HL and FA. The greatest difference is observed for the dosage f/b equal to 1.25, where a percentage difference of 99.99% is obtained in the values of $\xi_2$ when compared with the HL filler. Likewise, the sample with FA presents a 99.28% higher elasticity in contrast to the L filler.

Based on the lower dosage (f/b equal to 0.50), the model characterizes Young's modulus for the L filler with values different from those shown for the HL and FA fillers, which is directly related to the fineness of the filler used. In summary, the mathematical model is able to differentiate an elasticity $\xi_2$ for the type of filler at low concentrations (f/b equal to 0.50) only when there is a difference in the particle sizes as presented in this study (see Table 2).

When increasing the test temperature to 60 and 70 °C, the output $\xi_2$ values of the different mastics do not show large differences. Therefore, an ANOVA statistical analysis of the 10-cycle MSCR setting at 3.2 kPa is performed for all dosages and temperatures. Table 5 shows the values of the variance of parameter 2. It is obtained that the filler with HL and L presents a P-value of 99%, accepting the hypothesis that the elasticity $\xi_2$ of the type of filler is not affected when the temperature increases from 50 °C to 70 °C. In the case of FA, the elasticity obtained generates a greater dispersion of the data, obtaining a probability of success of 95.64%, which can be attributed to a possible chemical interaction between the filler/bitumen interface.

Fig. 9a shows the relationship between $J_{nr3.2}$ and $R_{3.2}$ for bitumen type B50/70 and asphalt mastics. The results indicate that with increasing temperature, higher $J_{nr}$ values are generated with lower recovery, due to the transformation from viscoelastic to the viscous state of the samples.

In particular, for a temperature of 50 °C, the mastics with L have the same $R_{3.2}$ range as the bitumen type B50/70 for f/b concentrations equal to 0.50–0.75. However, a mismatch is generated, obtaining lower creep deformations $J_{nr3.2}$, so it is necessary to calculate the $J_{nr}/R$ ratio to establish a performance index and quantify the elasticity of the fillers. Now, if the amount of $J_{nr}$ due to $R$ recovery is analyzed, it is observed that mastics with L filler present an improvement of 21–80% of $J_{nr}/R$ in comparison to bitumen type B50/70 for the variation f/b equal to 0.50–1.25f. In contrast, HL and FA fillers achieve an improvement between 78 and 99% and 59–95% respectively, determining better $J_{nr}/R$ ratios for the same f/b variation. Subsequently, as the temperature increases, greater differences are generated between mastics and bitumen, showing an increase in the $J_{nr}/R$ index of 91–99.93% for HL, 76–98% for FA and 60–89% for L filler in reference to bitumen type B50/70.

Fig. 9b shows a comparison between the results obtained in the LVE range with the damage obtained in the MSCR cumulative damage test for asphalt mastics. In relating these phenomena, it is necessary to specify that the parameter $|G^*|/\sin(\delta)$ is able to normalize an index for rutting failures for bitumens, but not for mastics ($|G^*|/\sin(\delta) > 1.00$ kPa). In this case, when comparing samples with fillers, it is observed that $|G^*||/\sin(\delta)$ has a significant influence due to temperature. In particular, the $|G^*||/\sin(\delta)$ and the reciprocal of $J_{nr3.2}$ have the same units (kPa) and when correlating their results for angular velocity 10 rad/s and temperatures of 50, 60 and 70 °C (see Fig. 6b), a good *Pearson* correlation of $\rho = 0.82$ is obtained, although not strong for p-value less than 0.05. This trend is generated due to the fact that independent of the test procedure, the samples decrease their stiffness as the test temperature increases, showing a higher value $\beta$ or softening. In the particular case for a test temperature, the samples increase their stiffness as the dosage f/b increases, but they soften as a result of the repetitive loads measured by $\beta$.

## 4. Conclusions

In the present investigation, the viscoelastic behaviour of asphalt mastics with three different types of fillers (HL, FA and L) at high and low temperatures analyzed using a DSR. The results obtained in this research demonstrate that the use of the rheological model proposed allows detailing the elastic capacity of the fillers and viscoelastic capacity of the bitumen for the multiple stress of the MSCR. The main conclusions of the study presented below:.

- The viscoelasticity model proposed in this paper represents a detailed way to mechanically characterize asphalt mastics. Unlike the classical viscoelastic models, the new proposed model allows detailing the elastic $\xi_2$ influence of the fillers, the viscoelasticity of the asphalt bitumen and its relationship with the f/b dosage used for an f/b range of 0.5 to 1.25.
- The use of fractional derivatives in the proposed model for the bitumen and asphalt mastics results in new terms in the MSCR test recovery modulus equation. The parameter $\beta$ explains more precisely the total energy release caused by the bitumen and mastic asphalt, quantifying the viscoelastic transition of the filler/bitumen system for the 10 cycles of 3.2 kPa, generating a study of the impact of the filler type and its relationship with the filler/bitumen dosage.
- The rheological analyses of the B50/70 type bitumen and the asphalt mastics have made it possible to quantify the effect of the fillers on the resulting mastics. The results obtained show that the samples with HL generate higher stiffness values $|G^*|$ and lower accumulated deformations $R$, compared to the FA filler, due to the greater fineness of its particles. In addition, a large development of the elastic capacity $\xi_2$ or Young's modulus is demonstrated, being directly proportional to the filler/bitumen ratio.
- In the future, further work is planned to obtain a complete design of asphalt mixtures, comparing the methodology of the present study with the development of bitumens, mastics and asphalt mixtures for fatigue and permanent deformation phenomena. This will help determine the influence of bitumen modifying materials on the behaviour of asphalt mastics.

## Declaration of Competing Interest

The authors declare that they have no known competing financial interests or personal relationships that could have appeared to influence the work reported in this paper.

*Acknowledgements*

The authors gratefully acknowledge the institutional support provided by the Vice-Rectory for Research, Development and Artistic Creation of the University Austral of Chile (VIDCA UACh), to the Santander Bank Iberoamerican Scholarship Program, and the pavements lab of the Faculty of Engineering Sciences. Besides, to the GITECO and GCS research groups from the University of Cantabria (Spain) for their support.

*Funding Sources*

This work was supported by the National Research and Development Agency (ANID) of Chile [FONDECYT Regular N°1211160] and [FONDECYT Regular N°1201029].

## Appendix A

In this appendix some examples of the problem discussed in the main text on the permanent deformations of bitumen B50/70 and the asphalt mastics studied are illustrate.

First, Eq. (10) is used to adjust the recovery phenomenon in the

bitumen at 50 °C in the 10 cycles independently (see Fig. 10). This procedure is achieved by means of computer codes using MATLAB©, defining the domain of elastic-viscous rheological properties of B50/70, $\xi_1$ and β respectively. The fractional derivative β is obtained as an indicator of the recoverable non-linear viscoelasticity, demonstrating the change between the elastic and viscous state (see Figs. 6, 7 and 8).

Once the B50/70 parameters have been obtained, the adjustment is defined by means of Eq. (11) (see Fig. 11) for the MSCR in asphalt mastics. For this adjustment, the elastic capacity of each filler ($\xi_2$) and its relation with the bitumen mass (f/b) are defined. The same procedure was used for all the combinations and temperatures studied.

## References


[1] M. Lagos-Varas, D. Movilla-Quesada, J.P. Arenas, A.C. Raposeiras, D. Castro-Fresno, M.A. Calzada-Pérez, A. Vega-Zamanillo, J. Maturana, Study of the mechanical behavior of asphalt mixtures using fractional rheology to model their viscoelasticity, Construction and Building Materials. 200 (2019) 124–134, https://doi.org/10.1016/j.conbuildmat.2018.12.073.

[2] A. Arabzadeh, H. Ceylan, S. Kim, A. Sassani, K. Gopalakrishnan, M. Mina, Electrically-conductive asphalt mastic: Temperature dependence and heating efficiency, Materials & Design. 157 (2018) 303–313, https://doi.org/10.1016/j.matdes.2018.07.059.

[3] M. Zaumanis, L.D. Poulikakos, M.N. Partl, Performance-based design of asphalt mixtures and review of key parameters, Materials & Design. 141 (2018) 185–201, https://doi.org/10.1016/j.matdes.2017.12.035.

[4] F. Russo, R. Veropalumbo, L. Pontoni, C. Oreto, S.A. Biancardo, N. Viscione, F. Pirozzi, M. Race, Sustainable asphalt mastics made up recycling waste as filler, Journal of Environmental Management. 301 (2022) 113826, https://doi.org/10.1016/j.jenvman.2021.113826.

[5] X. Zhu, Y. Yuan, L. Li, Y. Du, F. Li, Identification of interfacial transition zone in asphalt concrete based on nano-scale metrology techniques, Materials & Design. 129 (2017) 91–102, https://doi.org/10.1016/j.matdes.2017.05.015.

[6] M. Guo, A. Motamed, Y. Tan, A. Bhasin, Investigating the interaction between asphalt binder and fresh and simulated RAP aggregate, Materials & Design. 105 (2016) 25–33, https://doi.org/10.1016/j.matdes.2016.04.102.

[7] D. Movilla-Quesada, Á. Vega-Zamanillo, M.Á. Calzada-Pérez, D. Castro-Fresno, Evaluation of water effect on bituminous mastics with different contribution fillers and binders, Construction and Building Materials. 29 (2012) 339–347, https://doi.org/10.1016/j.conbuildmat.2011.08.093.

[8] J. Wang, M. Guo, Y. Tan, International Journal of Transportation Study on application of cement substituting mineral fillers in asphalt mixture, International Journal of Transportation Science and Technology. 7 (3) (2018) 189–198, https://doi.org/10.1016/j.ijtst.2018.06.002.

[9] D. Movilla-Quesada, O. Muñoz, A.C. Raposeiras, D. Castro-Fresno, Thermal suspectability analysis of the reuse of fly ash from cellulose industry as contribution filler in bituminous mixtures, Construction and Building Materials. 160 (2018) 268–277, https://doi.org/10.1016/j.conbuildmat.2017.11.046.

[10] A.K. Das, D. Singh, Investigation of rutting, fracture and thermal cracking behavior of asphalt mastic containing basalt and hydrated lime fillers, Construction and Building Materials. 141 (2017) 442–452, https://doi.org/10.1016/j.conbuildmat.2017.03.032.

[11] C. Li, Z. Chen, S. Wu, B.o. Li, J. Xie, Y. Xiao, Effects of steel slag fillers on the rheological properties of asphalt mastic, Effects of steel slag fillers on the rheological properties of asphalt mastic 145 (2017) 383–391, https://doi.org/10.1016/j.conbuildmat.2017.04.034.

[12] Y. Li, S. Liu, Z. Xue, W. Cao, Experimental research on combined effects of flame retardant and warm mixture asphalt additive on asphalt binders and bituminous mixtures, Construction and Building Materials. 54 (2014) 533–540, https://doi.org/10.1016/j.conbuildmat.2013.12.058.

[13] C.V. Phan, H. Di Benedetto, C. Sauzéat, D. Lesueur, S. Pouget, Influence of hydrated lime on linear viscoelastic properties of bituminous mastics, Mech Time-Depend Mater. 24 (1) (2020) 25–40, https://doi.org/10.1007/s11043-018-09404-x.

[14] K. Wu, K. Zhu, C. Kang, B. Wu, Z. Huang, An experimental investigation of flame retardant mechanism of hydrated lime in asphalt mastics, Materials & Design. 103 (2016) 223–229, https://doi.org/10.1016/j.matdes.2016.04.057.

[15] D. Lesueur, D.N. Little, Effect of Hydrated Lime on Rheology, Fracture, and Aging of Bitumen, Transportation Research Record. 1661 (1) (1999) 93–105, https://doi.org/10.3141/1661-14.

[16] É. Lachance-Tremblay, D. Perraton, M. Vaillancourt, H. Di Benedetto, Effect of hydrated lime on linear viscoelastic properties of asphalt mixtures with glass aggregates subjected to freeze-thaw cycles, Construction and Building Materials. 184 (2018) 58–67, https://doi.org/10.1016/j.conbuildmat.2018.06.130.

[17] F. Maghool, A. Arulrajah, Y.-J. Du, S. Horpibulsuk, A. Chinkulkijniwat, Environmental impacts of utilizing waste steel slag aggregates as recycled road construction materials Environmental impacts of utilizing waste steel slag aggregates as recycled road construction materials, Clean Technologies and Environmental Policy. 19 (4) (2017) 949–958, https://doi.org/10.1007/s10098-016-1289-6.

[18] A. Woszuk, L. Bandura, W. Franus, Fly ash as low cost and environmentally friendly filler and its effect on the properties of mix asphalt, Journal of Cleaner Production. 235 (2019) 493–502, https://doi.org/10.1016/j.jclepro.2019.06.353.

[19] R. Mistry, T. Kumar, Effect of using fly ash as alternative filler in hot mix asphalt, Perspectives in Science. 8 (2016) 307–309, https://doi.org/10.1016/j.pisc.2016.04.061.

[20] F. Li, Y. Yang, L. Wang, Evaluation of physicochemical interaction between asphalt binder and mineral filler through interfacial adsorbed film thickness, Construction and Building Materials. 252 (2020) 119135, https://doi.org/10.1016/j.conbuildmat.2020.119135.

[21] T. Ma, D. Zhang, Y. Zhang, Y. Zhao, X. Huang, Effect of air voids on the high-temperature creep behavior of asphalt mixture based on three-dimensional discrete element modeling, Materials & Design. 89 (2016) 304–313, https://doi.org/10.1016/j.matdes.2015.10.005.

[22] X. Ding, T. Ma, L. Gu, Y. Zhang, Investigation of surface micro-crack growth behavior of asphalt mortar based on the designed innovative mesoscopic test, Materials & Design. 185 (2020) 108238, https://doi.org/10.1016/j.matdes.2019.108238.

[23] M. Lagos-Varas, D. Movilla-Quesada, A.C. Raposeiras, J.P. Arenas, M.A. Calzada-Pérez, A. Vega-Zamanillo, P. Lastra-González, Influence of limestone filler on the rheological properties of bituminous mastics through susceptibility master curves, Construction and Building Materials. 231 (2020) 117126, https://doi.org/10.1016/j.conbuildmat.2019.117126.

[24] F. Safaei, C. Castorena, Material nonlinearity in asphalt binder fatigue testing and analysis, Materials & Design. 133 (2017) 376–389, https://doi.org/10.1016/j.matdes.2017.08.010.

[25] R.J. Jackson, A. Wojcik, M. Miodownik, 3D printing of asphalt and its effect on mechanical properties, Materials & Design. 160 (2018) 468–474, https://doi.org/10.1016/j.matdes.2018.09.030.

[26] M. Han, J. Li, Y. Muhammad, Y. Yin, J. Yang, S. Yang, S. Duan, Studies on the secondary modification of SBS modified asphalt by the application of octadecyl amine grafted graphene nanoplatelets as modifier, Diamond and Related Materials. 89 (2018) 140–150, https://doi.org/10.1016/j.diamond.2018.08.011.

[27] A. Jamshidi, M.O. Hamzah, K. Kurumisawa, T. Nawa, B. Samali, Evaluation of sustainable technologies that upgrade the binder performance grade in asphalt pavement construction, Materials & Design. 95 (2016) 9–20, https://doi.org/10.1016/j.matdes.2016.01.065.

[28] Y. Sun, W. Wang, J. Chen, Investigating impacts of warm-mix asphalt technologies and high reclaimed asphalt pavement binder content on rutting and fatigue performance of asphalt binder through MSCR and LAS tests, Journal of Cleaner Production. 219 (2019) 879–893, https://doi.org/10.1016/j.jclepro.2019.02.131.

[29] C. Wang, Y. Wang, Physico-chemo-rheological characterization of neat and polymer-modified asphalt binders, Construction and Building Materials. 199 (2019) 471–482, https://doi.org/10.1016/j.conbuildmat.2018.12.064.

[30] E. Dubois, D.Y. Mehta, A. Nolan, Correlation between multiple stress creep recovery (MSCR) results and polymer modification of binder, Construction and Building Materials. 65 (2014) 184–190, https://doi.org/10.1016/j.conbuildmat.2014.04.111.

[31] K. Hu, C. Yu, Q. Yang, Y. Chen, G. Chen, R. Ma, Multi–scale enhancement mechanisms of graphene oxide on styrene–butadiene–styrene modified asphalt: An exploration from molecular dynamics simulations, Materials & Design. 208 (2021) 109901, https://doi.org/10.1016/j.matdes.2021.109901.

[32] J. Zhang, L.F. Walubita, A.N.M. Faruk, P. Karki, G.S. Simate, Use of the MSCR test to characterize the asphalt binder properties relative to HMA rutting performance – A laboratory study, Construction and Building Materials. 94 (2015) 218–227, https://doi.org/10.1016/j.conbuildmat.2015.06.044.

[33] P. Li, X. Jiang, K. Guo, Y. Xue, H. Dong, Analysis of viscoelastic response and creep deformation mechanism of asphalt mixture, Construction and Building Materials. 171 (2018) 22–32, https://doi.org/10.1016/j.conbuildmat.2018.03.104.

[34] X. Zhu, Y. Sun, C. Du, W. Wang, J. Liu, J. Chen, Rutting and fatigue performance evaluation of warm mix asphalt mastic containing high percentage of artificial RAP binder, Construction and Building Materials. 240 (2020) 117860, https://doi.org/10.1016/j.conbuildmat.2019.117860.

[35] M. Lagos-Varas, A.C. Raposeiras, D. Movilla-Quesada, J.P. Arenas, D. Castro-Fresno, O. Muñoz-Cáceres, V.C. Andres-Valeri, Study of the permanent deformation of binders and asphalt mixtures using rheological models of fractional viscoelasticity, Construction and Building Materials. 260 (2020) 120438, https://doi.org/10.1016/j.conbuildmat.2020.120438.

[36] J. Zhang, C. Sun, P. Li, M. Liang, H. Jiang, Z. Yao, Experimental study on rheological properties and moisture susceptibility of asphalt mastic containing red mud waste as a filler substitute, Construction and Building Materials. 211 (2019) 159–166, https://doi.org/10.1016/j.conbuildmat.2019.03.252.

[37] E.-C. Tsardaka, M. Stefanidou, Study of the action of nano-alumina particles in hydrated lime pastes, Journal of Building Engineering. 46 (2022) 103808, https://doi.org/10.1016/j.jobe.2021.103808.

[38] H. Naveed, Z. ur Rehman, A. Hassan Khan, S. Qamar, M.N. Akhtar, Effect of mineral fillers on the performance, rheological and dynamic viscosity measurements of asphalt mastic, Construction and Building Materials. 222 (2019) 390–399, https://doi.org/10.1016/j.conbuildmat.2019.06.170.

[39] Q. Li, C. Zhu, H. Zhang, S. Zhang, Evaluation on long-term performance of emulsified asphalt cold recycled mixture incorporating fly ash by mechanistic and microscopic characterization, Construction and Building Materials. 319 (2022) 126120, https://doi.org/10.1016/j.conbuildmat.2021.126120.

[40] S. Xu, X. Liu, A. Tabaković, P. Lin, Y. Zhang, S. Nahar, B.J. Lommerts, E. Schlangen, The role of rejuvenators in embedded damage healing for asphalt pavement, Materials & Design. 202 (2021) 109564, https://doi.org/10.1016/j.matdes.2021.109564.

[41] Y. Zhang, M. van de Ven, A. Molenaar, S. Wu, Preventive maintenance of porous asphalt concrete using surface treatment technology, Materials & Design. 99 (2016) 262–272, https://doi.org/10.1016/j.matdes.2016.03.082.
[42] H. Zhang, K. Anupam, T. Scarpas, C. Kasbergen, S. Erkens, Contact mechanics based solution to predict modulus of asphalt materials with high porosities, Materials & Design. 206 (2021) 109752, https://doi.org/10.1016/j.matdes.2021.109752.
[43] Y. Gu, H.u. Wang, Y. Yu, Synchronization for commensurate Riemann-Liouville fractional-order memristor-based neural networks with unknown parameters, Journal of the Franklin Institute. 357 (13) (2020) 8870–8898, https://doi.org/10.1016/j.jfranklin.2020.06.025.
[44] H. Li, X. Luo, F. Ma, Y. Zhang, Micromechanics modeling of viscoelastic asphalt-filler composite system with and without fatigue cracks, Materials & Design. 209 (2021) 109983, https://doi.org/10.1016/j.matdes.2021.109983.
[45] C.F. Lorenzo, T.T. Hartley, Generalized functions for the fractional calculus, Glenn Research Center, National Aeronautics and Space Administration (NASA), 1999.
[46] X. Chen, W. Yang, X. Zhang, F. Liu, Unsteady boundary layer flow of viscoelastic MHD fluid with a double fractional Maxwell model, Applied Mathematics Letters. 95 (2019) 143–149, https://doi.org/10.1016/j.aml.2019.03.036.